

Identifying vital effects in *Halimeda* algae with Ca isotopes

C. L. Blättler^{1,*}, S. M. Stanley², G. M. Henderson¹, and H. C. Jenkyns¹

¹University of Oxford, Department of Earth Sciences, Oxford, UK

²University of Hawaii, Department of Geology & Geophysics, Honolulu, HI, USA

*now at Princeton University, Department of Geosciences, Princeton, NJ, USA

Correspondence to: C. L. Blättler
(blattler@princeton.edu)

Abstract. Geochemical records of biogenic carbonates provide some of the most valuable records of the geological past, but are often difficult to interpret without a mechanistic understanding of growth processes. In this experimental study, *Halimeda* algae are used as a test organism to untangle some of the specific factors that influence their skeletal composition, in particular their Ca-isotope composition. Algae were stimulated to precipitate both calcite and aragonite by growth in artificial Cretaceous seawater, resulting in experimental samples with somewhat malformed skeletons. The Ca-isotope fractionation of the algal calcite (−0.6‰) appears to be much smaller than that for the algal aragonite (−1.4‰), similar to the behaviour observed in inorganic precipitates. However, the carbonate from *Halimeda* has higher Ca-isotope ratios than inorganic forms by approximately 0.25‰, likely because of Rayleigh distillation within the algal intercellular space. In identifying specific vital effects and the magnitude of their influence on Ca-isotope ratios, this study suggests that mineralogy has a first-order control on the marine Ca-isotope cycle.

1 Introduction

This work investigates the mechanism of Ca-isotope fractionation in one of the major producers of aragonite sediment, *Halimeda* algae, to test models of biocalcification and the marine Ca-isotope cycle. Biogenic carbonate is the source of many important sedimentary records, which can be useful for interpreting ancient environments if the mechanisms of skeletal formation are understood. The elemental and isotopic compositions of biogenically precipitated minerals deviate from those of inorganic precipitates – differences sometimes referred to as “vital effects” – which complicate the application of geochemical proxies in skeletal material. Ca-isotope ratios, defined as $\delta^{44/40}\text{Ca}$

$= \left[\left(^{44}\text{Ca} / ^{40}\text{Ca} \right)_{\text{sample}} / \left(^{44}\text{Ca} / ^{40}\text{Ca} \right)_{\text{standard}} - 1 \right] \cdot 1000$, may provide a tool for understanding the environmental factors affecting carbonate geochemistry and are themselves a tool to assess past environmental conditions. Ca is the dominant cation in biogenic calcite and aragonite and should be subject to similar vital effects as other cations. The experiments presented here use skeletal material from 25 *Halimeda* to isolate particular aspects of the biocalcification process and quantify their effects on the Ca-isotope system.

Skeletal growth can be divided broadly into two categories, “biologically induced” and “biologically controlled”, reflecting the location of biomineralization, the transport of chemical species, and the influence of environmental conditions (Weiner and Dove, 2003). The green algae *Halimeda* spp. 30 are recognized as an example of a biologically induced system, based on the crystallography and organization of their aragonite needles (Borowitzka and Larkum, 1987) and confirmed by observation of changing skeletal mineralogy under experimental conditions (Stanley et al., 2010). Their simplicity provides an ideal starting point for addressing the mechanisms of cation fractionation in biogenically induced aragonite.

35 Samples for this study were generated in a controlled *Halimeda* growth experiment replicating the conditions of Stanley et al. (2010), where the Mg/Ca ratio of seawater was changed to reflect hypothetical conditions during Earth history. The current molar Mg/Ca ratio of the oceans is 5.2, which generally favours the precipitation of aragonite and high-Mg calcite (cation composition > 4 mol% Mg) over low-Mg calcite (cation composition < 4 mol% Mg), subject to favourable temperature conditions, $p\text{CO}_2$, phosphate, or sulfate concentrations (e.g. Burton and Walter, 1987, 1990; Morse et al., 1997; Bots et al., 2011). Several lines of evidence, such as halite fluid inclusions, nonskeletal carbonate mineralogy, and fossil echinoderm Mg/Ca, suggest that seawater Mg/Ca may have been as low as 1.0–1.5 during periods such as the Cretaceous, which would have favoured the precipitation of low-Mg calcite (Sandberg, 1983; Hardie, 1996; Stanley and Hardie, 1998; Lowenstein et al., 2001; 40 Horita et al., 2002; Dickson, 2004). Growth experiments on a variety of biocalcifiers under such low Mg/Ca conditions have produced changes in calcification rate and skeletal geochemistry (e.g. Stanley et al., 2002, 2005; Ries et al., 2006) and, in the case of *Halimeda incrassata*, a partial change in carbonate mineralogy from aragonite to calcite (Stanley et al., 2010). For this study, the *Halimeda* experiment was repeated with a close relative, *Halimeda discoidea*, to reproduce the unusual case of 45 aragonite and calcite grown simultaneously under the same conditions. The growth of two different carbonate minerals from the same bulk fluid presents a test case for the isotopic effects of carbonate mineral precipitation, modified by relatively simple algal biology, with implications for the balance of the Ca-isotope budget.

2 Background to Ca-isotope fractionation

55 2.1 Inorganic Ca-isotope fractionation

The behaviour of Ca isotopes in inorganic carbonates has been explored in a variety of precipitation experiments, with all calcium carbonate minerals expressing fractionation in favour of the lighter isotopes of Ca (see compilation in Fantle and Tipper, 2014). In isotope notation, this is expressed as $\alpha < 1$ (where α is the ratio of precipitate $^{44}\text{Ca}/^{40}\text{Ca}$ to solution $^{44}\text{Ca}/^{40}\text{Ca}$) or $\Delta^{44/40}\text{Ca} < 0$ (where $\Delta^{44/40}\text{Ca}$ is equal to $\delta^{44/40}\text{Ca}_{\text{carbonate}} - \delta^{44/40}\text{Ca}_{\text{solution}}$). Fractionation of laboratory-grown aragonite ($\Delta^{44/40}\text{Ca}$) has an average value of -1.7‰ at 15 °C , while showing a small positive temperature dependence of 0.015‰ per $^{\circ}\text{C}$ (Gussone et al., 2003). Smaller fractionations are generally observed during calcite growth, with samples precipitated in a beaker averaging -0.8‰ at 15 °C , with a similar positive temperature dependence as for aragonite (Marriott et al., 2004). Much greater fractionations, up to -2.34‰ , have been observed in laboratory speleothem-like calcite growth (Reynard et al., 2011), and relationships between $\Delta^{44/40}\text{Ca}$ and other factors such as growth rate and $[\text{CO}_3^{2-}]$ have also been identified (Lemarchand et al., 2004; Tang et al., 2008). Gussone et al. (2011) showed that the metastable CaCO_3 polymorph ikaite expresses smaller fractionations of -0.55‰ and -0.62‰ for experimental and natural samples, respectively, grown between 0 and 6 °C , while laboratory-grown vaterite has an even smaller average fractionation of -0.36‰ at temperatures between 10 and 48 °C . Measured fractionations of less than -0.2‰ for synthetic amorphous calcium carbonate (ACC) suggest that Ca-isotope ratios are not strongly affected in the absence of a mineral structure (Gagnon et al., 2011), although the cause of isotopic offsets for the different carbonate minerals is not understood.

75 Models of Ca-isotope fractionation suggest that the preference for light isotopes in solid mineral phases is due to a kinetic effect associated with ion dehydration and attachment onto a surface, moderated by the kinetic fractionations of a backwards detachment reaction and ion transport effects (Gussone et al., 2003; DePaolo, 2011). The isotopic fractionation between fluid and carbonate in equilibrium appears to be close to zero, based on evidence from pore fluids and deep-sea carbonate sediment (Fantle and DePaolo, 2007) and from groundwater and host rock in a long-lived carbonate aquifer (Jacobson and Holmden, 2008). These observations suggest that maximum fractionation occurs at intermediate growth rates when isotopically light surface-layer ions are incorporated into the crystal, and ion transport in the fluid is rapid enough not to limit the expression of the attachment fractionation (DePaolo, 2011). This model can explain the relationships between $\delta^{44/40}\text{Ca}$ and several growth variables as observed during inorganic precipitation experiments (e.g. Lemarchand et al., 2004; Tang et al., 2008), but it may not translate directly to biological settings.

2.2 Biogenic Ca-isotope fractionation

In biological calcification systems, carbonate skeletons are also isotopically lighter than the fluid (usually seawater) from which they precipitate, but the degree of fractionation and responses to variable growth conditions differ from the inorganic data presented above, confirming the presence of vital effects (e.g. Gussone et al., 2003, 2006; Böhm et al., 2006). For example, temperature changes induce a range of responses in various marine organisms. Many forms of biogenic carbonate exhibit a similar temperature dependence to that of inorganic precipitates of 0.01–0.03 ‰ per °C (e.g. Gussone et al., 2003, 2005; Böhm et al., 2006; Gussone et al., 2006), although there are significant exceptions to this trend. The planktic foraminifera *G. sacculifer* and *N. pachyderma* express much greater sensitivities of 0.22–0.24 ‰ per °C (Nägler et al., 2000; Hippler et al., 2006) and 0.17 ‰ per °C (Hippler et al., 2009), respectively, although subsequent studies of these and other planktic foraminifera show a negligible temperature dependence (Chang et al., 2004; Sime et al., 2005; Griffith et al., 2008; Kasemann et al., 2008). A study of benthic foraminifera revealed a temperature sensitivity of ~0.02 ‰ per °C for shells formed at temperatures > 5 °C, but deviations from this relationship at temperatures < 5 °C (Gussone and Filipsson, 2010). Very large Ca-isotope ranges (1.6 to 3.7 ‰) were found within individual foraminiferal shells on the scale of 10s of microns using in situ secondary ion mass spectrometry (Rollion-Bard et al., 2007; Kasemann et al., 2008). These different responses in biocalcifiers, in contrast to the relatively consistent temperature sensitivity of inorganic carbonates, demonstrate that metabolic or physiological processes can contribute significantly to skeletal $\delta^{44/40}\text{Ca}$ and indicate the potential for Ca isotopes to provide information about the processes of biominerization.

Isotopic vital effects are also observed in response to carbonate-ion concentration and growth rate. A strong correlation with both $[\text{CO}_3^{2-}]$ and growth rate was observed for inorganic calcite (Lemarchand et al., 2004), but no correlation was apparent with $[\text{CO}_3^{2-}]$ for the planktic foraminifera *O. universa* (Gussone et al., 2005) nor several coccolithophorid species (Gussone et al., 2006, 2007; Langer et al., 2007). Growth rate was shown to have an effect on $\delta^{44/40}\text{Ca}$ in the planktic foraminifera *G. siphonifera* (Kısakürek et al., 2011), but not for the coccolithophore *E. huxleyi* (Langer et al., 2007). Observed variations in skeletal $\delta^{44/40}\text{Ca}$ in response to salinity may also be related to changes in growth rate, given that assemblages are usually adapted to local salinity conditions and are stressed by environmental changes (Gussone et al., 2009; Kısakürek et al., 2011). These studies suggest that Ca-isotope responses to $[\text{CO}_3^{2-}]$ and growth rate are determined by biological control over internal pH and carbonate chemistry, and are likely to vary according to specific biocalcification mechanisms.

Estimating the precise magnitude of vital effects in biocalcifiers is complicated by the additional isotopic fractionations associated with ion reservoirs and fractional utilization of Ca. The blue mussel, *Mytilus edulis*, demonstrates the significance of these effects by precipitating its skeleton from an extra-pallial fluid that has higher $\delta^{44/40}\text{Ca}$ than the surrounding seawater (Heinemann et al., 2008), producing a difference in $\delta^{44/40}\text{Ca}$ between its calcitic and aragonitic skeletal components of only

0.25 ‰, rather than the expected 0.9 ‰ for an inorganic process. Transport effects and Rayleigh distillation have also been implicated in coccolith calcification (Gussone et al., 2006) and coral skeletal growth (Böhm et al., 2006). For foraminifera, conflicting estimates of the magnitude of these internal isotopic fractionations have been made, balancing their utilization of an internal pool of Ca against its compositional difference from seawater (Erez, 2003; Gussone et al., 2009). Griffith et al. (2008) developed a Ca-isotope model ($\alpha = 0.9985$, 85 % utilization) suggesting that this internal reservoir could be offset by -0.8 to -0.9 ‰ from seawater, whereas Kısakürek et al. (2011) proposed that utilization of only 10–40 % of the reservoir indicates a smaller offset of -0.2 to -0.4 ‰, with additional fractionation originating from active Ca-pumping. Before proxy $\delta^{44/40}\text{Ca}$ measurements can be linked to environmental variables, the magnitudes and relative contributions of these competing biological and physico-chemical effects must be resolved.

135 3 Samples and methods

3.1 *Halimeda* experiment

This case study investigates the balance of isotopic effects linked to specific biocalcification mechanisms in the sample organism, *Halimeda discoidea*. Experiments were performed at the University of Hawai‘i to induce the growth of both calcite and aragonite from the normally aragonitic algae, 140 essentially replicating the previous experimental conditions of Stanley et al. (2010), which showed clear aragonite needles and calcite rhombs in SEM images. Individual specimens of *Halimeda discoidea* were collected offshore Hawai‘i from a sandy substrate at a depth of ~ 1.5 m off the coast of Waimanalo, Oahu. They were transported within less than one hour in a two-gallon container containing their ambient seawater to an aquarium containing 30 L of artificial seawater with the ionic 145 chemistry of modern seawater and maintained at 25 ± 1 °C. They were planted by burying their hold-fasts in sand, positioning them as they had been in nature. They were illuminated and fertilized as described for previous experiments with *Halimeda* (Stanley et al., 2010). After being acclimated in that aquarium for one week, they were transferred to an aquarium that was identical to the one in which they were acclimated, except that the molar Mg/Ca ratio was maintained at 1.5 and $[\text{Ca}^{2+}]$ at 150 25.3 mM, while the sum of $([\text{Mg}^{2+}] + [\text{Ca}^{2+}])$ remained equal to that of modern seawater to match total salinity. After approximately six weeks of growth, eight individuals were harvested, rinsed thoroughly in distilled water, and sent to the University of Oxford (Figure 3). The samples look rather different than wild specimens, likely because of the stressed growth conditions under low Mg/Ca and limited time for full growth and calcification.

155 A number of wild specimens were also analyzed to compare with the experimental samples. Various species of *Halimeda* algae (see Table 1) were collected in the vicinity of Lee Stocking Island in the Bahamas. The sampling locality was in shallow water (ca. 1 m) on the leeward side of a barrier island close to the coast.

3.2 Sample preparation

160 Four to five terminal segments from each individual *Halimeda* were sampled by hand and washed three times in 18 MΩ water to remove dried sea salt. Samples were then bleached for 1 hour using ~15 % NaClO and an ultrasonication bath to remove organic matter. Following this treatment, samples were rinsed five times in 10 MΩ water, patted dry and air-dried completely overnight, and crushed to a powder by mortar and pestle. The same homogenized powders were used for both XRD (X-ray diffractometry) and Ca-isotope analysis. Test analyses of untreated, washed, and bleached *Halimeda* indicate that these methods do not affect the mineralogy or isotopic results, aside from removal of a halite signal from the XRD spectrum. Estimates of the skeletal mass fraction were derived from comparison of the mass of powder to the amount of dissolved carbonate, as determined by measuring the concentration of Ca in solution and assuming a skeletal composition of pure stoichiometric CaCO₃.

170

3.3 XRD analysis

X-ray diffractometry (XRD) was used to quantify the percentage of calcite and aragonite in each sample using a PANalytical X'Pert Pro diffractometer in the Department of Chemistry, University of Oxford. Approximately 10 mg of sample powder was scattered onto a glass slide with a frosted 175 surface to randomize particle orientation. Analyses used a Cu-K α X-ray source (40 mA and 40 kV) with the sample loaded on a fixed stage while 2 θ varied through 25–40° with a 0.004° step size (0.05° s⁻¹). Aragonite produces prominent peaks at 2 θ = 26.2° (3.40 Å, [111]), 27.2° (3.27 Å, [021]), and 33.0° (2.70 Å, [012]), whereas calcite produces a much stronger relative signal at 2 θ = 29.4° (3.04 Å, [104]). The dominant calcite peak has a greater magnitude than that of any aragonite peak 180 for a mass contribution of only 10 % calcite. For the purpose of assessing the mass fraction of carbonate minerals, a calibration curve was generated using mixtures of aragonite (a fire coral, *Millepora*, from the Bahamas) and calcite (mineral spar) standards. The proportion of calcite was calculated using areas under the aragonite peak at 2 θ = 26.2° and the calcite peak at 2 θ = 29.4° and the formula % cc = cc/(cc + arag) (Figure 1) along with a curve fit to the data. Errors for determination of % cc 185 are estimated to be 5 %, based on the scatter of the standard calibration curve.

3.4 Ca-isotope analysis

Ca-isotope analysis by multi-collector inductively coupled plasma mass spectrometry (MC-ICP-MS) was performed on both carbonates and growth solutions, using between 0.5 and 2.0 mg of carbonate 190 powder. Methods are derived from those in Blättler et al. (2011). Sample Ca was isolated using ion-exchange chromatographic columns and prepared as 10 ppm Ca solutions in 2 % HNO₃, with blanks contributing < 5 ng Ca to the total sample. Ratios of ⁴⁴Ca/⁴²Ca were measured on a Nu Instruments MC-ICP-MS with standard–sample–standard bracketing, with the international carbonate

standard NIST SRM915a used as a reference (Eisenhauer et al., 2004). Mass-dependent fractionation was confirmed by measuring ^{44}Ca , ^{43}Ca , and ^{42}Ca beams, correcting for the interference of double-charged Sr by monitoring the beam at mass 43.5. Multiple internal standard measurements and replicate analyses of samples generate standard errors of $\sim 0.05\text{‰}$ (external precision). Values of $\delta^{44/42}\text{Ca}$, equal to $\left[\left(\frac{^{44}\text{Ca}}{^{42}\text{Ca}}\right)_{\text{sample}} / \left(\frac{^{44}\text{Ca}}{^{42}\text{Ca}}\right)_{\text{standard}} - 1\right] \cdot 1000$ relative to the standard SRM 915a, are converted to $\delta^{44/40}\text{Ca}$ relative to modern seawater using a $\delta^{44/40}\text{Ca}$ value of 1.88 for seawater relative to SRM915a (Hippler et al., 2003). and $\Delta^{44/40}\text{Ca}$ (Table 1). $\Delta^{44/40}\text{Ca}$ are calculated by subtracting $\delta^{44/40}\text{Ca}$ of the growth fluid from that of the carbonate (Table 1).

4 Results

The growth experiment yielded *Halimeda* skeletons which contained small amounts of calcite, although the proportions of calcite were not as significant as in a previous experiment (Stanley et al., 2010). Whereas the carbonate skeleton of natural, wild samples contained 0–5 % calcite, seven of the experimental samples had slightly increased levels of 2.8–8.8 % calcite (Table 1, Figure 2). The eighth experimental individual (Sample #6) was poorly calcified and its XRD spectrum had a very weak calcite peak and no visually identifiable aragonite peak. Peak area calculations resulted in a calculated % calcite of 88 %, but this value is probably affected by the background noise levels during XRD analysis and best treated as a minimum. This sample is therefore treated as having a skeletal mineralogy of > 85 % calcite with an estimated error of up to 15 %.

The quantitative mineralogical data are consistent with the morphologies of the experimental *Halimeda*, with the lowest amounts of calcite (within the range of natural *Halimeda*) present in thick, well-calcified segments, whereas higher levels (up to 8.8 %) were present in flimsier, malformed samples (Figure 3). All the specimens were somewhat less calcified than natural, wild-grown specimens, which is a result of the limited growth interval of the experiment. The most calcite-rich sample was particularly shriveled and yielded a skeletal mass fraction < 10 % of total sample mass, in comparison to other experimental and natural algae where the skeletons represented 45–75 % of the total mass.

Ca-isotope ratios of various experimental materials were measured to establish $\Delta^{44/40}\text{Ca}$, the difference between fluid and precipitate, for all samples (Table 1, Figure 4). Analyses include the calcium chloride salt added to the aquarium water, the aquarium water from both before and after the growth period, terminal algal samples which grew entirely in artificial Cretaceous–Eocene seawater (eight individual *Halimeda*), and basal algal samples whose calcification commenced in natural seawater and may have continued in experimental seawater after transplanting (three individuals). The Ca in the artificial seawater was a mixture of modern seawater Ca and added calcium chloride salt in an approximate proportion of 1 : 3, based on the $\delta^{44/40}\text{Ca}$ of seawater (0 ‰, as the reference value), the salt (−1.19 ‰), and the resulting solution (−0.87 ‰). The Ca-isotope ratio in

the aquarium appears to have risen slightly (by +0.1‰) during the course of the experiment, which may be due to analytical error or to the preferential uptake of light Ca isotopes during the growth period. This would imply significant removal of Ca (~10 %) from the aquarium during the experiment, which could be the result of both algal calcification and/or abiotic precipitation on other surfaces in the aquarium, but would not result in a large effect on the $\delta^{44/40}\text{Ca}$ fractionation of carbonate precipitation.

The seven experimental algae with < 10 % calcite had an average $\delta^{44/40}\text{Ca}$ of -2.31‰ relative to natural seawater, or $\Delta^{44/40}\text{Ca} = -1.44\text{\textperthousand}$. This fractionation is in good agreement with six natural *Halimeda* samples which express $\Delta^{44/40}\text{Ca} = -1.42\text{\textperthousand}$. Variability on the order of 0.3‰ is present within both of these sample groups. Three samples taken from the base of the experimental algae, rather than the terminal segments which grew entirely in the aquarium, had an average $\delta^{44/40}\text{Ca}$ of -1.65‰ relative to natural seawater, reflecting a mixture of carbonate precipitated before the transplant and continued calcification from the isotopically lighter aquarium water. The anomalous, calcite-rich sample had a much smaller fractionation than other *Halimeda*, with $\delta^{44/40}\text{Ca}$ of -1.47‰ and $\Delta^{44/40}\text{Ca} = -0.61\text{\textperthousand}$. This sample, although only a single specimen, provides the opportunity to test the relationship between skeletal mineralogy and Ca-isotope fractionation of *Halimeda*. The discussion below treats this sample as a possible indicator for the effect of calcite in *Halimeda*, but further experiments that reproduce these effects would be recommended to establish the results with more certainty.

5 Discussion

The identification of specific fractionation mechanisms in the *Halimeda* Ca-isotope data is possible due to the relatively simple biology of the algae. *Halimeda* grow by initially forming a white proto-segment which is then populated with chloroplasts the next day, and begins calcification with aragonite needles soon after active photosynthesis commences (Larkum et al., 2011). The rapid calcification of *Halimeda* allows it to be a major contributor to modern carbonate mud (Neumann and Lynton, 1975). During the process of aragonite growth, *Halimeda* exert minimal control on the calcification process and the environment in which it takes place. Calcium carbonate oversaturation is achieved by photosynthetic CO₂ consumption and subsequent local CO₃²⁻ elevation, without additional control over the carbonate system (Borowitzka and Larkum, 1987). Cell walls provide surfaces for precipitation of aragonite needles which subsequently fill the intercellular space, and their morphology suggests that the algae do not further control the crystallography of the precipitate with organic templates (Borowitzka and Larkum, 1987; Macintyre and Reid, 1995). Insensitivity to Ca-channel blocking drugs indicates that algal tissue has no influence on the supply of Ca, leaving diffusion of seawater as the only uptake mechanism (de Beer and Larkum, 2001). This lack of biological cation transport is consistent with the observation of similar Mg/Ca ratios for inorganic

precipitates and *Halimeda* during experiments in solutions with a variety of Mg/Ca ratios (Stanley et al., 2010). Without the complicating effects of organic matrices and active transport observed in 265 some biological systems, the simplicity of *Halimeda* skeletal formation makes it possible to focus on other specific factors affecting Ca-isotope ratios.

Under these conditions for precipitation, the presence of different carbonate polymorphs can help define the influence of mineralogy on the chemical composition of skeletal carbonate in *Halimeda*. While clearly defined mineralogical changes were not as evident in these experiments as for the 270 experiments of Stanley et al. (2010), the single, calcite-rich sample with a much smaller $\Delta^{44/40}\text{Ca}$ is suggestive and begs explanation. One tempting explanation for this data is that the experimental *Halimeda* reflect a calcite–aragonite mixing line, which can be used to define endmember Ca-isotope values for the pure calcite and pure aragonite phases (Fig. 5). The offset in $\delta^{44/40}\text{Ca}$ between aragonite and calcite endmembers is nearly identical, at ca. 0.9‰, for both the experimental *Halimeda* 275 and inorganic precipitates, suggesting that the intrinsic fractionation factor for these carbonate polymorphs is expressed even when these crystals are formed in biogenic settings. It is perhaps unexpected that this relationship should have a similar slope to the mixing line between inorganic phases, due to the possibility of competing isotopic effects from changes in growth rate, for example. Although a range of $\Delta^{44/40}\text{Ca}$ values have been observed for calcite and aragonite, the consistent offset 280 between the phases suggests that effects from growth rate or CO_3^{2-} content are secondary to the first-order relationship between mineralogy and $\Delta^{44/40}\text{Ca}$. Given this behaviour for Ca-isotope ratios in this study, it would be expected that other metal/Ca ratios experience a similarly strong influence from carbonate mineralogy in *Halimeda* skeletons. While this interpretation relies heavily on a single sample to define the calcite–aragonite mixing line, the Mg/Ca data in Stanley et al. (2010) also 285 support the hypothesis that *Halimeda* skeletal geochemistry strongly reflects the inorganic chemistry of the preferred carbonate mineral.

These *Halimeda* data also allow the effect of substrate on Ca-isotope fractionation to be assessed. Beaker experiments usually probe carbonate-nucleated growth of calcite or aragonite, but understanding the effect of an organic substrate on carbonate geochemistry could be important for interpreting 290 ooid or microbial mat carbonate. The *Halimeda* experiment is able to isolate this factor to some degree, due to the space and manner in which aragonite needles grow (Borowitzka and Larkum, 1987). The results suggest that the organic substrate may be important for determining carbonate mineralogy, but not for further affecting cation geochemistry. The prevalence of aragonite in most of the experimental *Halimeda*, despite a fluid composition that mimics Cretaceous seawater (molar Mg/Ca=1.5) and strongly favours calcite, suggests that the cell walls exerted influence 295 over carbonate mineralogy, even without a three-dimensional organic matrix. By influencing the mineralogy of the first nucleated crystals, the organic surface may affect the structure and therefore geochemistry of further growth, even when the ambient fluid promotes an alternative mineralogy. *Halimeda* appears to behave in this manner, and other carbonate associated with, but not entirely

300 controlled by, organic material may show similar mineralogical and geochemical behaviour.

Although many aspects of *Halimeda* calcification resemble inorganic calcification, $\Delta^{44/40}\text{Ca}$ for *Halimeda* over the observed range of mineralogical compositions is $\sim 0.25\text{\textperthousand}$ smaller than for inorganic precipitates in the experiments of Gussone et al. (2003) and Marriott et al. (2004). Among the several factors which could introduce a vital effect of this magnitude, the calcification process 305 of *Halimeda* suggests two primary candidates for this difference. One possibility is increased carbonate saturation and calcification rate, which has been shown to decrease fractionation on both an experimental and theoretical basis (Lemarchand et al., 2004; DePaolo, 2011). Within the intercellular spaces, consumption of CO_2 by photosynthesis drives carbonate oversaturation and promotes calcification. However, differences in calcification rate were visibly apparent in the samples, which 310 ranged from thick and fleshy to stunted and shriveled, and did not always accompany changes in $\delta^{44/40}\text{Ca}$. This relationship implies that growth rate had a minor impact on Ca-isotope ratios. The second possibility is the occurrence of Rayleigh distillation, or a reservoir effect. As light isotopes are preferentially consumed within the intercellular space, the $\delta^{44/40}\text{Ca}$ of that reservoir will rise and the apparent fractionation between the external fluid and the skeleton will decrease. The rate of 315 calcification relative to the recharge of Ca ions into the calcifying space by diffusion would determine the magnitude of this effect. The observed enrichment of $\sim 0.25\text{\textperthousand}$ for the integrated product of Rayleigh distillation implies removal of 25 % of the Ca within the reservoir, given the inorganic fractionation factor of $-1.7\text{\textperthousand}$. This mechanism could be responsible for the difference in $\Delta^{44/40}\text{Ca}$ of inorganic aragonite and aragonitic sponges, as the sponges also have a simple system of induced biocalcification (Gussone et al., 2005). Although the balance of calcification to diffusion rate 320 could be specific to individual organisms, some inherent link between the two could arise as DIC (dissolved inorganic carbon) supply eventually limits calcification. If such a link occurs in other settings, then the magnitude of the Rayleigh effect in *Halimeda*, $\sim 0.25\text{\textperthousand}$, may reflect a characteristic vital effect among macroorganisms with a similar calcification mechanism.

325 The Ca-isotope fractionation that is expressed by *Halimeda* has implications for the marine Ca-isotope budget. Due to the large difference in $\Delta^{44/40}\text{Ca}$ between aragonite and calcite, it is possible that the overall proportion of these two minerals in the global carbonate sink can affect the steady-state Ca-isotope composition of seawater (Farkaš et al., 2007; Blättler et al., 2012). This mechanism can help explain variation in reconstructed seawater $\delta^{44/40}\text{Ca}$ over the Phanerozoic only if the difference 330 between sedimentary aragonite and calcite $\delta^{44/40}\text{Ca}$ is maintained over time. Although few major calcifying species remained quantitatively important contributors to the carbonate sink over long timescales (10^7 – 10^8 years), and *Halimeda* only became a major sediment producer in the late Cenozoic aragonite sea (Stanley and Hardie, 1998), the first-order control of mineralogy on biogenic $\delta^{44/40}\text{Ca}$ in this experimental setup appears to support this hypothesis.

335 **6 Conclusions**

This work presents a growth experiment with the sediment-producing algae *Halimeda* that investigates mechanisms of biocalcification and their geochemical expression. Developing a mechanistic understanding of biogenic carbonate formation and associated vital effects is necessary for linking skeletal proxy measurements to environmental interpretations and mass-balance calculations. While 340 not applicable to every calcifying organism, the principles derived here show that it is possible to understand a combination of factors with superimposed effects on skeletal geochemistry. The inferred relationship between mineralogy and Ca-isotope ratios for the experimental *Halimeda* demonstrate how mineralogy strongly influences Ca-isotope ratios in biominerals. Biological substrates can exert first-order control on Ca-isotope fractionation by promoting a particular mineral form. The most 345 substantial vital effect in this example is likely to be Rayleigh distillation of Ca within the algal intercellular space, which may have analogues in other simple macroorganisms. Stronger vital effects in other biocalcifiers are likely due to more sophisticated ion-transport mechanisms and internal reservoir dynamics, but the expression of an intrinsic mineralogical signal within *Halimeda* suggests that the calcite and aragonite content of marine carbonate can significantly affect the Ca-isotope balance 350 of seawater. Further work on this and other biocalcifiers may continue to unravel the factors that control carbonate composition and increase the value of these important geological archives.

Acknowledgements. Thanks are due to Jennifer Engels for harvesting and shipping experimental samples to Oxford, Phil Holdship for analyzing cation concentrations in experimental seawater, and Phil Wiseman for generously accommodating XRD analyses in the Department of Chemistry, University of Oxford. This work 355 was significantly improved following detailed comments by anonymous reviewers, and the authors wish to acknowledge those contributions with thanks.

References

Blättler, C. L., Jenkyns, H. C., Reynard, L. M., and Henderson, G. M.: Significant increases in global weathering during Oceanic Anoxic Events 1a and 2 indicated by calcium isotopes, *Earth and Planetary Science Letters*, 360 309, 77–88, doi:10.1016/j.epsl.2011.06.029, 2011.

Blättler, C. L., Henderson, G. M., and Jenkyns, H. C.: Explaining the Phanerozoic Ca-isotope history of seawater, *Geology*, 40, 843–846, doi:10.1130/G33191.1, 2012.

Böhm, F., Gussone, N., Eisenhauer, A., Dullo, W.-C., Reynaud, S., and Paytan, A.: Calcium isotope fractionation in modern scleractinian corals, *Geochimica et Cosmochimica Acta*, 70, 4452–4462, 365 doi:10.1016/j.gca.2006.06.1546, 2006.

Borowitzka, M. A. and Larkum, A. W. D.: Calcification in algae: mechanisms and the role of metabolism, *Critical Reviews in Plant Sciences*, 6, 1–45, doi:10.1080/07352688709382246, 1987.

Bots, P., Benning, L. G., Rickaby, R. E. M., and Shaw, S.: The role of SO_4 in the switch from calcite to aragonite seas, *Geology*, 39, 331–334, 2011.

Burton, E. A. and Walter, L. M.: Relative precipitation rates of aragonite and Mg calcite from seawater: Temperature or carbonate ion control?, *Geology*, 15, 111–114, 1987.

Burton, E. A. and Walter, L. M.: The role of pH in phosphate inhibition of calcite and aragonite precipitation rates in seawater, *Geochimica et Cosmochimica Acta*, 54, 797–808, 1990.

Chang, V. T.-C., Williams, R. J. P., Makishima, A., Belshaw, N. S., and O'Nions, R. K.: Mg and Ca isotope fractionation during CaCO_3 biomineralisation, *Biochemical and Biophysical Research Communications*, 323, 375 79–85, doi:10.1016/j.bbrc.2004.08.053, 2004.

de Beer, D. and Larkum, A. W. D.: Photosynthesis and calcification in the calcifying algae *Halimeda discoidea* studied with microsensors, *Plant, Cell and Environment*, 24, 1209–1217, doi:10.1046/j.1365-3040.2001.00772.x, 2001.

DePaolo, D. J.: Surface kinetic model for isotopic and trace element fractionation during precipitation of calcite from aqueous solutions, *Geochimica et Cosmochimica Acta*, 75, 1039–1056, doi:10.1016/j.gca.2010.11.020, 380 2011.

Dickson, J. A. D.: Echinoderm skeletal preservation: calcite–aragonite seas and the Mg/Ca ratio of Phanerozoic oceans, *Journal of Sedimentary Research*, 74, 355–365, doi:10.1306/112203740355, 2004.

Eisenhauer, A., Nägler, T. F., Stille, P., Kramers, J., Gussone, N., Bock, B., Fietzke, J., Hippler, D., and Schmitt, 385 A.-D.: Proposal for international agreement on Ca notation resulting from discussions at workshops on stable isotope measurements held in Davos (Goldschmidt 2002) and Nice (EGS-AGU-EUG 2003), *Geostandards and Geoanalytical Research*, 28, 149–151, doi:10.1111/j.1751-908X.2004.tb01051.x, 2004.

Erez, J.: The source of ions for biomineralization in foraminifera and their implications for paleoceanographic proxies, *Reviews in Mineralogy and Geochemistry*, 54, 115–149, doi:10.2113/0540115, 2003.

Fantle, M. S. and DePaolo, D. J.: Ca isotopes in carbonate sediment and pore fluid from ODP Site 807A: The $\text{Ca}^{2+}(\text{aq})$ –calcite equilibrium fractionation factor and calcite recrystallization rates in Pleistocene sediments, *Geochimica et Cosmochimica Acta*, 71, 2524–2546, doi:10.1016/j.gca.2007.03.006, 2007.

Fantle, M. S. and Tipper, E. T.: Calcium isotopes in the global biogeochemical Ca cycle: Implications for development of a Ca isotope proxy, *Earth-Science Reviews*, 129, 148–177, doi:10.1016/j.earscirev.2013.10.004, 395 2014.

Farkaš, J., Böhm, F., Wallmann, K., Blenkinsop, J., Eisenhauer, A., van Geldern, R., Munnecke, A., Voigt, S., and Veizer, J.: Calcium isotope record of Phanerozoic oceans: Implications for chemical evolution of seawater and its causative mechanisms, *Geochimica et Cosmochimica Acta*, 71, 5117–5134, 400 doi:10.1016/j.gca.2007.09.004, 2007.

Gagnon, A. C., DePaolo, D. J., Adkins, J. F., and De Yoreo, J. J.: Calcium isotopes during coral biomineralization, in: Goldschmidt Conference Abstracts, vol. 75, p. 880, *Mineralogical Magazine*, 2011.

Griffith, E. M., Paytan, A., Kozdon, R., Eisenhauer, A., and Ravelo, A. C.: Influences on the fractionation of calcium isotopes in planktonic foraminifera, *Earth and Planetary Science Letters*, 268, 124–136, 405 doi:10.1016/j.epsl.2008.01.006, 2008.

Gussone, N. and Filipsson, H. L.: Calcium isotope ratios in calcitic tests of benthic foraminifers, *Earth and Planetary Science Letters*, 290, 108–117, doi:10.1016/j.epsl.2009.12.010, 2010.

Gussone, N., Eisenhauer, A., Heuser, A., Dietzel, M., Bock, B., Böhm, F., Spero, H. J., Lea, D. W., Bijma, J., and Nägler, T. F.: Model for kinetic effects on calcium isotope fractionation ($\delta^{44}\text{Ca}$) in inorganic aragonite and cultured planktonic foraminifera, *Geochimica et Cosmochimica Acta*, 67, 1375–1382, 410 doi:10.1016/S0016-7037(02)01296-6, 2003.

Gussone, N., Böhm, F., Eisenhauer, A., Dietzel, M., Heuser, A., Teichert, B. M. A., Reitner, J., Wörheide, G., and Dullo, W.-C.: Calcium isotope fractionation in calcite and aragonite, *Geochimica et Cosmochimica Acta*, 69, 4485–4494, doi:10.1016/j.gca.2005.06.003, 2005.

Gussone, N., Langer, G., Thoms, S., Nehrke, G., Eisenhauer, A., Riebesell, U., and Wefer, G.: Cellular calcium pathways and isotope fractionation in *Emiliania huxleyi*, *Geology*, 34, 625–628, doi:10.1130/G22733.1, 415 2006.

Gussone, N., Langer, G., Geisen, M., Steel, B. A., and Riebesell, U.: Calcium isotope fractionation in coccoliths of cultured *Calcidiscus leptoporus*, *Helicosphaera carteri*, *Syracosphaera pulchra* and *Umbilicosphaera foliosa*, *Earth and Planetary Science Letters*, 260, 505–515, doi:10.1016/j.epsl.2007.06.001, 2007.

Gussone, N., Hönisch, B., Heuser, A., Eisenhauer, A., Spindler, M., and Hemleben, C.: A critical evaluation of calcium isotope ratios in tests of planktonic foraminifers, *Geochimica et Cosmochimica Acta*, 73, 7241–7255, doi:10.1016/j.gca.2009.08.035, 2009.

Gussone, N., Nehrke, G., and Teichert, B. M. A.: Calcium isotope fractionation in ikaite and vaterite, *Chemical Geology*, 285, 194–202, doi:10.1016/j.chemgeo.2011.04.002, 2011.

Hardie, L. A.: Secular variation in seawater chemistry: An explanation for the coupled secular variation in the mineralogies of marine limestones and potash evaporites over the past 600 m.y., *Geology*, 24, 279–283, doi:10.1130/0091-7613(1996)024<0279:SVISCA>2.3.CO;2, 1996.

Heinemann, A., Fietzke, J., Eisenhauer, A., and Zumholz, K.: Modification of Ca isotope and trace metal 430 composition of the major matrices involved in shell formation of *Mytilus edulis*, *Geochemistry Geophysics Geosystems*, 9, Q01 006, doi:10.1029/2007GC001777, 2008.

Hippler, D., Schmitt, A.-D., Gussone, N., Heuser, A., Stille, P., Eisenhauer, A., and Nägler, T. F.: Calcium isotopic composition of various reference materials and seawater, *Geostandards Newsletter*, 27, 13–19, doi:10.1111/j.1751-908X.2003.tb00709.x, 2003.

Hippler, D., Eisenhauer, A., and Nägler, T. F.: Tropical Atlantic SST history inferred from Ca isotope thermometry over the last 140ka, *Geochimica et Cosmochimica Acta*, 70, 90–100, doi:10.1016/j.gca.2005.07.022, 435

2006.

Hippler, D., Kozdon, R., Darling, K. F., Eisenhauer, A., and Nägler, T. F.: Calcium isotopic composition of high-latitude proxy carrier *Neogloboquadrina pachyderma* (sin.), *Biogeosciences*, 6, 1–14, doi:10.5194/bg-440 6-1-2009, 2009.

Holmden, C., Papanastassiou, D. A., Blanchon, P., and Evans, S.: $\delta^{44/40}\text{Ca}$ variability in shallow water carbonates and the impact of submarine groundwater discharge on Ca-cycling in marine environments, *Geochimica et Cosmochimica Acta*, 83, 179–194, doi:10.1016/j.gca.2011.12.031, 2012.

Horita, J., Zimmermann, H., and Holland, H. D.: Chemical evolution of seawater during the Phanerozoic: 445 Implications from the record of marine evaporites, *Geochimica et Cosmochimica Acta*, 66, 3733–3756, doi:10.1016/S0016-7037(01)00884-5, 2002.

Jacobson, A. D. and Holmden, C.: $\delta^{44}\text{Ca}$ evolution in a carbonate aquifer and its bearing on the equilibrium isotope fractionation factor for calcite, *Earth and Planetary Science Letters*, 270, 349–353, doi:10.1016/j.epsl.2008.03.039, 2008.

450 Kasemann, S. A., Schmidt, D. N., Pearson, P. N., and Hawkesworth, C. J.: Biological and ecological insights into Ca isotopes in planktic foraminifers as a palaeotemperature proxy, *Earth and Planetary Science Letters*, 271, 292–302, doi:10.1016/j.epsl.2008.04.007, 2008.

Kisakürek, B., Eisenhauer, A., Böhm, F., Hathorne, E. C., and Erez, J.: Controls on calcium isotope fractionation in cultured planktic foraminifera, *Globigerinoides ruber* and *Globigerinella siphonifera*, *Geochimica et 455 Cosmochimica Acta*, 75, 427–443, doi:10.1016/j.gca.2010.10.015, 2011.

Langer, G., Gussone, N., Nehrke, G., Riebesell, U., Eisenhauer, A., and Thoms, S.: Calcium isotope fractionation during coccolith formation in *Emiliania huxleyi*: Independence of growth and calcification rate, *Geochemistry Geophysics Geosystems*, 8, Q05 007, doi:10.1029/2006GC001422, 2007.

460 Larkum, A. W. D., Salih, A., and Kühl, M.: Rapid mass movement of chloroplasts during segment formation of the calcifying siphonalean green alga, *Halimeda macroloba*, *PLoS ONE*, 6, e20 841, doi:10.1371/journal.pone.0020841, 2011.

Lemarchand, D., Wasserburg, G. J., and Papanastassiou, D. A.: Rate-controlled calcium isotope fractionation in synthetic calcite, *Geochimica et Cosmochimica Acta*, 68, 4665–4678, doi:10.1016/j.gca.2004.05.029, 2004.

465 Lowenstein, T. K., Timofeeff, M. N., Brennan, S. T., Hardie, L. A., and Demicco, R. V.: Oscillations in Phanerozoic seawater chemistry: evidence from fluid inclusions, *Science*, 294, 1086–1088, doi:10.1126/science.1064280, 2001.

Macintyre, I. G. and Reid, R. P.: Crystal alteration in a living calcareous alga (*Halimeda*): implications for studies in skeletal diagenesis, *Journal of Sedimentary Research*, 65, 143–153, doi:10.1306/D4268054-2B26-11D7-8648000102C1865D, 1995.

470 Marriott, C. S., Henderson, G. M., Belshaw, N. S., and Tudhope, A. W.: Temperature dependence of $\delta^7\text{Li}$, $\delta^{44}\text{Ca}$ and Li/Ca during growth of calcium carbonate, *Earth and Planetary Science Letters*, 222, 615–624, doi:10.1016/j.epsl.2004.02.031, 2004.

Morse, J. W., Wang, Q., and Tsio, M. Y.: Influences of temperature and Mg: Ca ratio on CaCO_3 precipitates from seawater, *Geology*, 25, 85–87, 1997.

475 Nägler, T. F., Eisenhauer, A., Müller, A., Hemleben, C., and Kramers, J.: The $\delta^{44}\text{Ca}$ -temperature calibration on fossil and cultured *Globigerinoides sacculifer*: New tool for reconstruction of past sea surface temperatures,

Geochemistry Geophysics Geosystems, 1, 1052, doi:10.1029/2000GC000091, 2000.

Neumann, A. C. and Lynton, S. L.: Lime mud deposition and calcareous algae in the Bight of Abaco, Bahamas: A budget, *Journal of Sedimentary Petrology*, 45, 763–786, 1975.

480 Reynard, L. M., Day, C. C., and Henderson, G. M.: Large fractionation of calcium isotopes during cave-analogue calcium carbonate growth, *Geochimica et Cosmochimica Acta*, 75, 3726–3740, doi:10.1016/j.gca.2011.04.010, 2011.

Ries, J. B., Stanley, S. M., and Hardie, L. A.: Scleractinian corals produce calcite, and grow more slowly, in artificial Cretaceous seawater, *Geology*, 34, 525–528, doi:10.1130/G22600.1, 2006.

485 Rollion-Bard, C., Vigier, N., and Spezzaferri, S.: In situ measurements of calcium isotopes by ion microprobe in carbonates and application to foraminifera, *Chemical Geology*, 244, 679–690, doi:10.1016/j.chemgeo.2007.07.021, 2007.

Sandberg, P. A.: An oscillating trend in Phanerozoic non-skeletal carbonate mineralogy, *Nature*, 305, 19–22, doi:10.1038/305019a0, 1983.

490 Sime, N. G., De La Rocha, C. L., and Galy, A.: Negligible temperature dependence of calcium isotope fractionation in 12 species of planktonic foraminifera, *Earth and Planetary Science Letters*, 232, 51–66, doi:10.1016/j.epsl.2005.01.011, 2005.

Stanley, S. M. and Hardie, L. A.: Secular oscillations in the carbonate mineralogy of reef-building and sediment-producing organisms driven by tectonically forced shifts in seawater chemistry, *Palaeogeography, Palaeoclimatology, Palaeoecology*, 144, 3–19, doi:10.1016/S0031-0182(98)00109-6, 1998.

495 Stanley, S. M., Ries, J. B., and Hardie, L. A.: Low-magnesium calcite produced by coralline algae in seawater of Late Cretaceous composition, *Proceedings of the National Academy of Sciences*, 99, 15 323–15 326, doi:10.1073/pnas.232569499, 2002.

Stanley, S. M., Ries, J. B., and Hardie, L. A.: Seawater chemistry, coccolithophore population growth, and the 500 origin of Cretaceous chalk, *Geology*, 33, 593–596, doi:10.1130/G21405.1, 2005.

Stanley, S. M., Ries, J. B., and Hardie, L. A.: Increased production of calcite and slower growth for the major sediment-producing alga *Halimeda* as the Mg/Ca ratio of seawater is lowered to a “calcite sea” level, *Journal of Sedimentary Research*, 80, 6–16, doi:10.2110/jsr.2010.011, 2010.

Tang, J., Dietzel, M., Böhm, F., Köhler, S. J., and Eisenhauer, A.: $\text{Sr}^{2+}/\text{Ca}^{2+}$ and $^{44}\text{Ca}/^{40}\text{Ca}$ fractionation 505 during inorganic calcite formation: II. Ca isotopes, *Geochimica et Cosmochimica Acta*, 72, 3733–3745, doi:10.1016/j.gca.2008.05.033, 2008.

Weiner, S. and Dove, P. M.: An overview of biomineralization processes and the problem of the vital effect, *Reviews in Mineralogy and Geochemistry*, 54, 1–29, doi:10.2113/0540001, 2003.

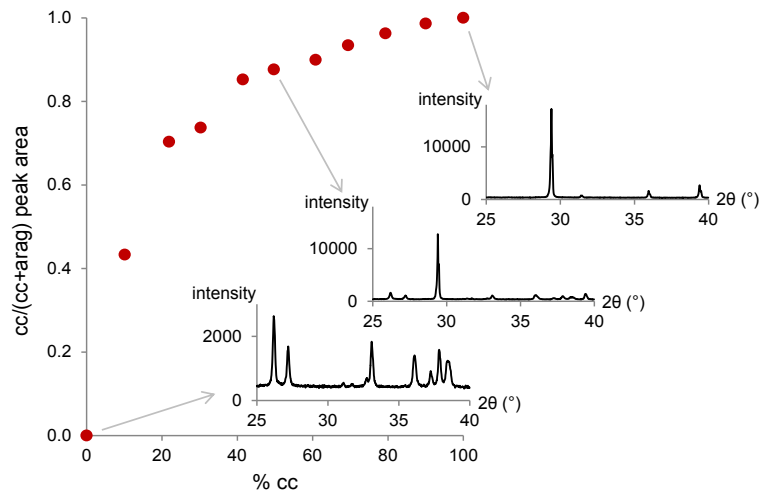


Fig. 1. Standard calibration curve for quantifying the proportions of calcite and aragonite using XRD. Analyses used a Cu-K α X-ray source (40 mA and 40 kV) with the sample loaded on a fixed stage while 2θ varied through 25–40° with a 0.004° step size (0.05°s^{-1}). Areas under the calcite (cc) peak at 29.4° and the aragonite (arag) peak at 26.2° were used to calculate the proportional intensity of calcite as $\text{cc}/(\text{cc} + \text{arag})$. Insets show standard intensity vs. 2θ -angle XRD spectra for 0 % (pure aragonite), 49.7 %, and 100 % calcite (note the relative change in the vertical axis for the 0 % calcite/pure aragonite standard).

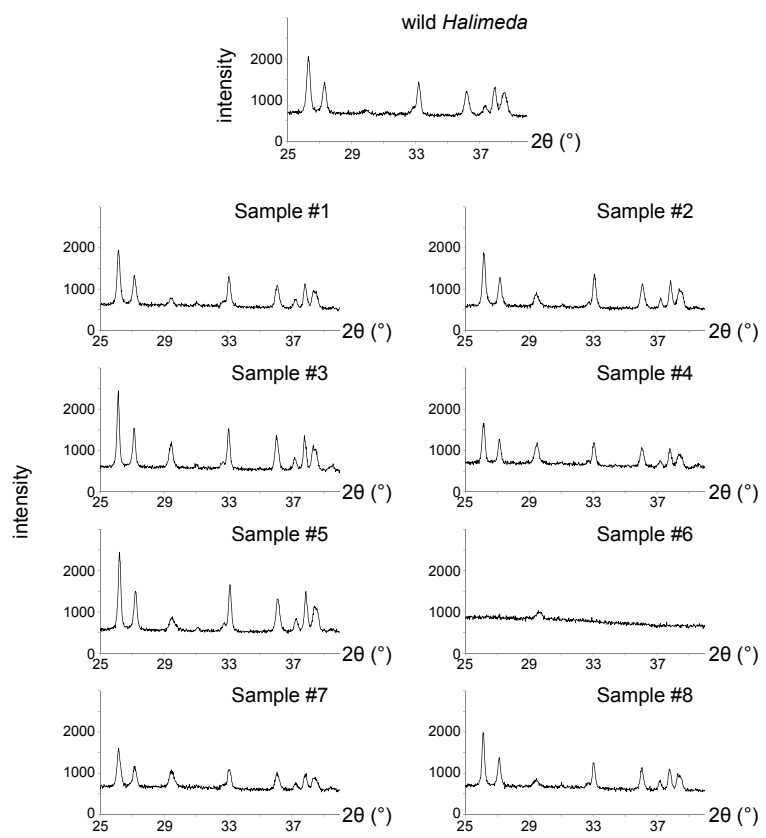


Fig. 2. XRD spectra of the experimental *Halimeda* and a wild specimen. Note the small calcite peak and lack of aragonite peaks present for Sample #6.



wild *Halimeda discoidea*



Sample #1, 2.8% cc



Sample #2, 4.9% cc



Sample #3, 7.6% cc



Sample #4, 8.8% cc



Sample #5, 3.7% cc



Sample #6, >88% cc



Sample #7, 8.5% cc



Sample #8, 4.0% cc*

*offshoot, grown

entirely in aquarium

Fig. 3. Photographs of the eight individual *Halimeda* samples from the experimental Cretaceous seawater. Note that Sample #6, which contained mostly calcite rather than aragonite, appears particularly malformed.

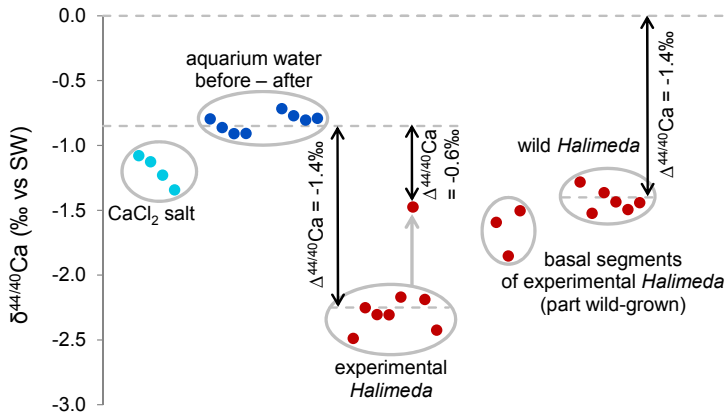


Fig. 4. Ca-isotope data from the *Halimeda* experiment as well as wild *Halimeda* measured in this study. Note that $\Delta^{44/40}\text{Ca}$ values, the offsets between growth medium and skeleton, are similar for the majority of the experimental and wild *Halimeda*, despite different $\delta^{44/40}\text{Ca}$ values.

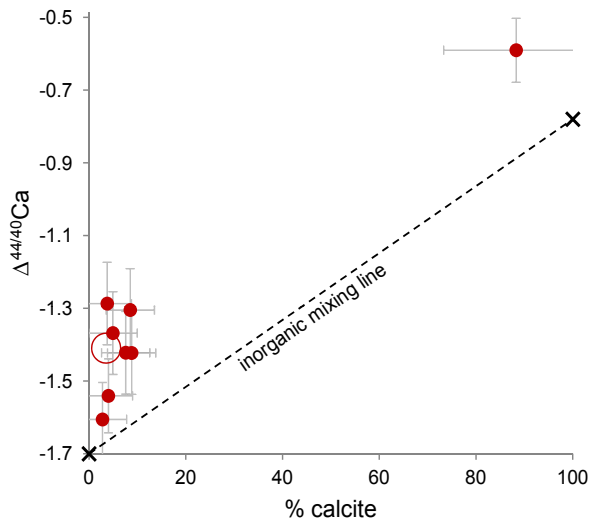


Fig. 5. Ca-isotope ratios for *Halimeda* grown in experimental Cretaceous seawater, plotted against the percentage of calcite determined by XRD analysis. The open circle represents the average value for natural, ocean-grown *Halimeda*. The black line represents a mixing relationship between the inorganic calcite and aragonite end-members from Marriott et al. (2004) and Gussone et al. (2005), respectively, at 15 °C. The *Halimeda* data occupy a region of similar slopes and approximately 0.25‰ heavier values than inorganic carbonate.

Table 1. Ca-isotope and mineralogical data for natural and experimental *Halimeda* algae and other experimental materials. Percent calcite (% cc) determined by XRD.

Sample name	$\delta^{44/42}\text{Ca} (\text{\textperthousand})$ rel. to SRM915a	n	$\delta^{44/40}\text{Ca} (\text{\textperthousand})$ rel. to seawater	2 SE	avg. $\delta^{44/40}\text{Ca}$	$\Delta^{44/40}\text{Ca}$	% cc	wt.% carbonate
Ca salt used for Cretaceous “seawater”								
CaCl ₂ -A	0.40	4	-1.08	0.07	-1.19			
CaCl ₂ -B	0.38	4	-1.13	0.07				
CaCl ₂ -C	0.33	4	-1.23	0.10				
CaCl ₂ -D	0.27	3	-1.34	0.11				
Pre-experimental Cretaceous “seawater”								
PRE-A	0.54	4	-0.80	0.07	-0.87	0.00		
PRE-B	0.51	4	-0.86	0.07				
PRE-C	0.49	4	-0.91	0.10				
PRE-D	0.49	3	-0.91	0.11				
Post-experimental Cretaceous “seawater”								
EXP-A	0.58	4	-0.72	0.07	-0.77	0.10		
EXP-B	0.55	4	-0.77	0.07				
EXP-C	0.54	3	-0.81	0.10				
EXP-D	0.54	4	-0.79	0.11				
Experimental <i>Halimeda</i> samples, post-XRD analysis (terminal segments only)								
HAL-1	-0.30	5	-2.49	0.10	-2.20	-1.62	2.8	73
HAL-2	-0.19	4	-2.25	0.11		-1.38	4.9	70
HAL-3	-0.21	4	-2.31	0.11		-1.44	7.6	63
HAL-4	-0.21	4	-2.31	0.11		-1.44	8.8	49
HAL-5	-0.15	4	-2.17	0.11		-1.30	3.7	57
HAL-6*	0.20	4	-1.47	0.09		-0.61	88.3	4
HAL-7	-0.15	4	-2.19	0.11		-1.32	8.5	45
HAL-8**	-0.27	5	-2.42	0.10		-1.56	4.0	50
Transplanted <i>Halimeda</i> samples (basal samples)								
HAL-2X	0.14	5	-1.59	0.09	-1.65	-1.59		
HAL-4X	0.01	5	-1.85	0.09		-1.85		
HAL-6X	0.19	5	-1.50	0.09		-1.50		
Wild <i>Halimeda</i> samples (from the Bahamas)								
<i>H. monile</i>	0.30	4	-1.28	0.13	-1.42	-1.28		
<i>H. tuna</i>	0.18	4	-1.52	0.13		-1.52		
<i>H. discoidea</i>	0.26	4	-1.36	0.13		-1.36	1.6	
<i>H. discoidea</i>	0.22	4	-1.44	0.13		-1.44		
<i>H. incrassata</i>	0.19	4	-1.50	0.13		-1.50		
<i>H. incrassata</i>	0.22	4	-1.44	0.13		-1.44		
Wild <i>Halimeda</i> samples (from Punta Maroma, Mexico, after Holmden et al. (2012))								
<i>H. opuntia</i>			-1.22		-1.18	-1.22		
<i>H. tuna</i>			-1.22			-1.22		
<i>H. incrassata</i>			-1.11			-1.11		

* poorly calcified sample

** offshot of another individual, entirely grown in aquarium